ACCOUNTS
of chemical research

Advanced Solid-State NMR Approaches for Structure Determination of Membrane Proteins and Amyloid Fibrils

MING TANG, GEMMA COMELLAS, AND CHAD M. RIENSTRA*

Department of Chemistry, University of Illinois at Urbana−Champaign, 600 South Mathews Avenue, Urbana, Illinois 61801, United States

RECEIVED ON JANUARY 24, 2013

CONSPECTUS

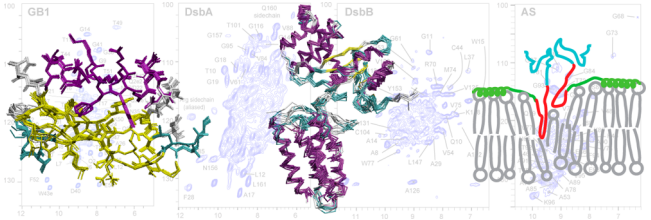

Solid-state NMR (SSNMR) spectroscopy has become an important technique for studying the biophysics and structure biology of proteins. This technique is especially useful for insoluble membrane proteins and amyloid fibrils, which are essential for biological functions and are associated with human diseases. In the past few years, as major contributors to the rapidly advancing discipline of biological SSNMR, we have developed a family of methods for high-resolution structure determination of microcrystalline, fibrous, and membrane proteins. Key developments include order-of-magnitude improvements in sensitivity, resolution, instrument stability, and sample longevity under data collection conditions. These technical advances now enable us to apply new types of 3D and 4D experiments to collect atomic-resolution structural restraints in a site-resolved manner, such as vector angles, chemical shift tensors, and internuclear distances, throughout large proteins.

In this Account, we present the technological advances in SSNMR approaches towards protein structure determination. We also describe the application of those methods for large membrane proteins and amyloid fibrils. Particularly, the SSNMR measurements of an integral membrane protein DsbB support the formation of a charge-transfer complex between DsbB and ubiquinone during the disulfide bond transfer pathways. The high-resolution structure of the DsbA−DsbB complex demonstrates that the joint calculation of X-ray and SSNMR restraints for membrane proteins with low-resolution crystal structure is generally applicable. The SSNMR investigations of α-synuclein fibrils from both wild type and familial mutants reveal that the structured regions of α-synuclein fibrils include the early-onset Parkinson's disease mutation sites. These results pave the way to understanding the mechanism of fibrillation in Parkinson's disease.

Introduction

Emerging magic-angle spinning (MAS) solid-state NMR (SSNMR) methods provide a new and innovative approach to address the protein structure determination problem. SSNMR allows for a wide variety of sample preparations to be utilized in order to study protein structures. Over the past decade, biomolecular SSNMR has progressed significantly from studying small peptides to solving high-resolution structures of large protein aggregates. A major push of our research focus over the past few years has been to develop methodologies enabling SSNMR structures to be fully determined with a sufficient quality and quantity of restraints to result in unique structures that are consistent with all experimental data and define the position of all heavy atoms to <1 Å RMSD. Here we review the technology development of SSNMR MAS techniques as well as the application for the assignment and structure determination of membrane proteins and amyloid fibrils.

Technology Development

A major distinguishing characteristic of our work is the emphasis upon 3D recoupling experiments to obtain highly precise and accurate structural parameters in a site-resolved fashion throughout entire proteins. For example, our 3D

Published on the Web 05/10/2013 www.pubs.acs.org/accounts
10.1021/ar4000168 © 2013 American Chemical Society

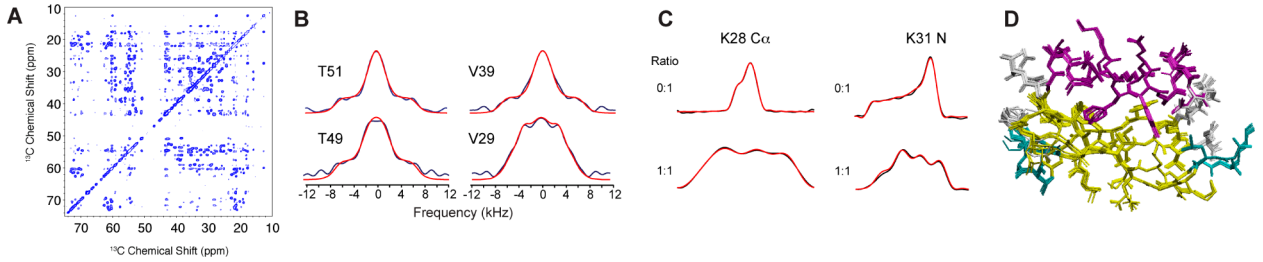

FIGURE 1. High-resolution SSNMR structure of GB1. (A) 2D $^{13}C-^{13}C$ correlation spectra of 1,3-^{13}C-glycerol labeled GB1.[4] Peak intensities are interpreted semiempirically in terms of internuclear distances. (B) Dipolar line shapes from 3D dipolar-shift correlation spectra of GB1, used to derive VEAN restraints.[4] Experimental HN-HACA line shapes (blue) were fit to simulations of the spin dynamics (red), as a function of the relative orientation of the two ^{1}H-X dipole vectors. (C) Dipolar:CST correlation spectra for both $^{13}C\alpha$ and ^{15}N sites of GB1.[8] Experimental spectra are presented in black, with simulations in red. Ratios provided are the ratio of dipolar to CST evolution. (D) The 10 lowest-energy structures of GB1 calculated using all CST information, vector angles, TALOS dihedrals, and all distances.[8] The backbone RMSD is 0.16 Å, and all heavy atom RMSD is 0.72 Å. Adapted with permission from refs 4 and 8. Copyright 2007 National Academy of Sciences.

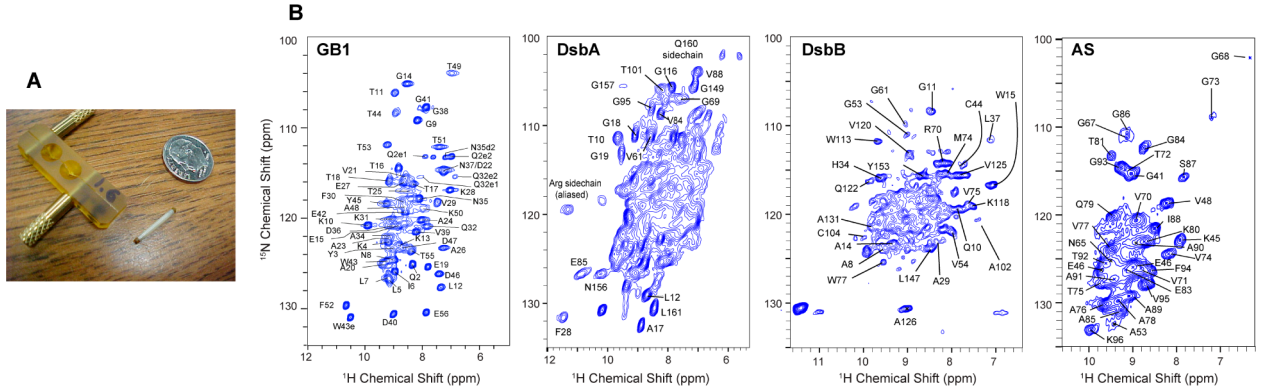

FIGURE 2. ^{1}H-detected SSNMR spectroscopy of deuterated proteins. (A) 1.6 mm SSNMR rotor which can contain ~5 mg of material and spin up to 40 kHz MAS. (B) $^{15}N-^{1}H$ 2D spectra of deuterated proteins: GB1, DsbA, membrane protein DsbB, and α-synuclein (AS) fibrils.[13,14] Adapted with permission from refs 13 and 14. Copyright 2007 John Wiley & Sons, Inc. and 2011 Springer Science + Business Media, respectively.

methods for measuring vector angles via correlated dipolar evolution yield angular restraints of a few degrees precision (Figure 1B).[1] Chemical shift anisotropy (CSA)-recoupling methods provide site-resolved tensor parameters (Figure 1C), related directly to high-resolution backbone structure.[2] We have developed SSNMR methods to enhance the sensitivity and resolution by 4D SSNMR,[3] and to obtain structural restraints such as internuclear distances,[4] vector angles (VEAN),[1,4] chemical shift tensors (CST),[2,5−8] and TEDOR heteronuclear distances.[9] Together with these techniques, we have solved the highest resolution structure of the B1 Ig binding domain of protein G (GB1) so far determined by SSNMR[4] and further refined it to a resolution of better than 0.2 Å RMSD (Figure 1D),[8] which compares favorably to 1 Å crystal structures. These capabilities pave the way for the structure determination of more difficult membrane proteins and amyloid fibrils.

^{1}H-Detection SSNMR by Fast MAS. We have made major advances in optimizing both the hardware and software required for executing ^{1}H-detection methods for membrane proteins and amyloid fibrils. We have developed FastMAS probe technology[10−13] and a suite of ^{1}H-dectection pulse sequences,[14] extending the range of proteins amenable to such methods. These techniques not only provide higher resolution ^{1}H spectra, but also enable the examination of proteins with much smaller volume MAS rotors (8 μL, Figure 2A). Thus, we have achieved significant sensitivity enhancement (~20-fold, or 400 times faster in terms of time)[11] through ^{1}H-detection experiments, using our FastMAS probe in combination with new solvent suppression pulse sequences[10] and triply (^{2}H,^{13}C,^{15}N) labeled protein samples. With the high spectral resolution and sensitivity from the fast MAS conditions at 750 MHz, we acquired semiquantitative $^{1}H-^{1}H$ distance restraints in a series of 3D experiments, and together these data were used (with TALOS[15]) to generate the first complete structure of a solid protein determined with ^{1}H-detected distances. The combination of spin dilution, high field (750 MHz), fast MAS (39 kHz), and triple resonance experiments enabled hundreds of ^{15}N- and ^{13}C-resolved $^{1}H-^{1}H$ distance restraints to

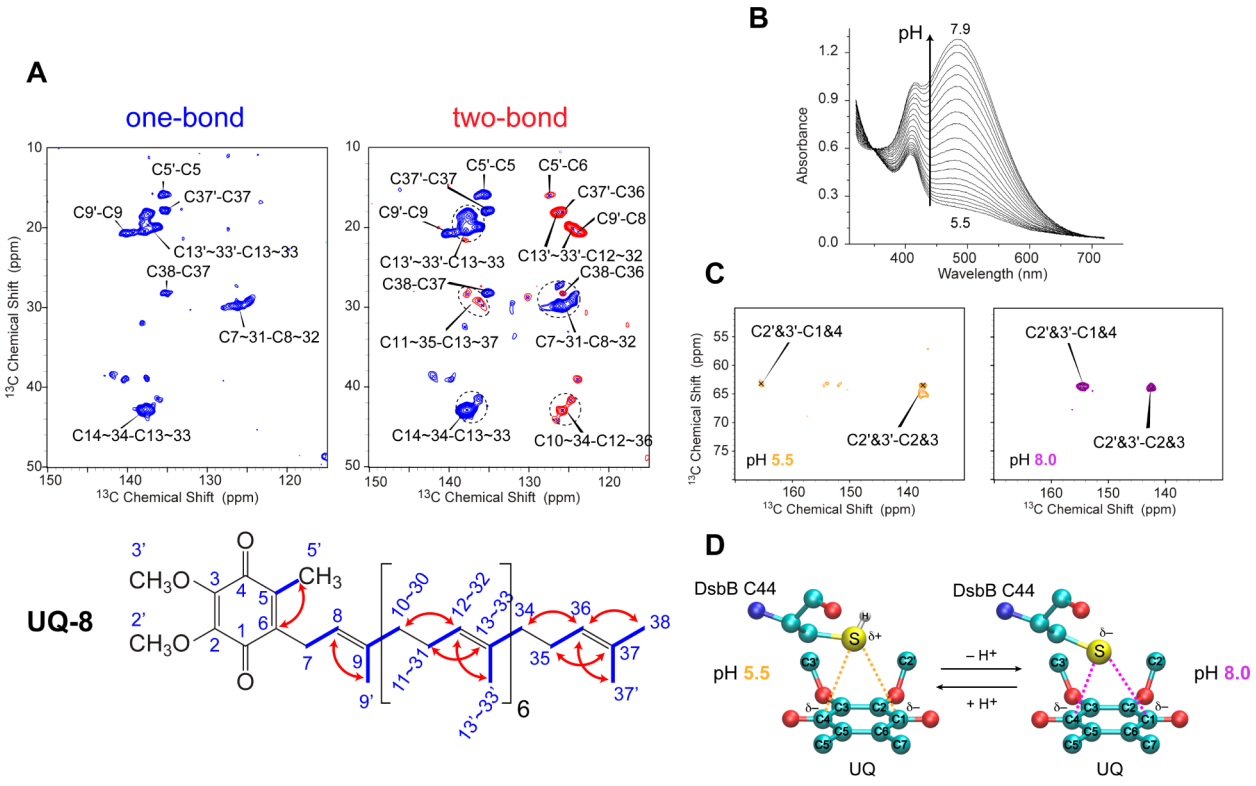

FIGURE 3. DsbB–UQ-8 interactions.[32] (A) $^{13}C-^{13}C$ DQ spectra of U–^{13}C, ^{15}N-DsbB(C41S). Blue contours represent one-bond correlations, and red contours represent two-bond correlations with the opposite sign. UQ-8 structure with highlights of one-bond (blue lines) and two-bond (red arrows) correlations observed in DQ experiments. (B) UV–vis spectra of DsbB(C41S) from pH 5.5 to 7.9. C44 pK_a is 6.6 by data fitting. (C) UQ resonances in the $^{13}C-^{13}C$ 2D correlation spectra of reversely labeled-DsbB(C41S) samples at pH 5.5 and 8.0. (D) Schematic representations of DsbB C44 and UQ complex at pH 5.5 (left) and pH 8.0 (right). Atoms are color-coded: carbons (cyan), oxygens (red), sulfurs (yellow), hydrogen (white), and nitrogens (blue). Dashed lines indicate the interactions between thiolate/thiol and UQ carbonyl groups. Adapted with permission from ref 32. Copyright 2011 American Chemical Society.

be obtained, which were integrated into the structure calculation.[13] So far, we have applied the ^1H-detection methods to a variety of deuterated protein samples, such as microcrystalline GB1, microcrystalline DsbA, membrane protein DsbB, and α-synuclein (AS) fibrils (Figure 2B).[14]

Membrane Proteins

Atomic-resolution structures of proteins advance our understanding of fundamental biological processes behind pathogenesis and provide a basis for rational design of therapeutics. Membrane proteins (MP) are especially important targets for structure elucidation, because they carry out many essential biological functions and thereby are targeted by ~60% of drugs.[16] However, MPs are extraordinarily difficult to study in vitro.[17−23] Interrogating the structure of MPs hinges on the ability to identify optimal conditions for expression, purification, crystallization, and/or solubilization for NMR. Relatively few MP structures have been determined,[18] and often the structures have moderate-to-low resolution (~2.5–4.0 Å) and/or missing or disordered portions, such as active site prosthetic groups. There are (November 2012) 371 unique MP structures in the PDB (http://blanco.biomol.uci.edu/mpstruc/listAll/list). Many hundreds of additional MPs can be expressed and purified, but do not diffract with sufficient quality to solve atomic-resolution structures. Such MPs, accumulating at this bottleneck in the structure determination pipeline, are potentially suitable for new and improved NMR methodologies. SSNMR methods can be applied in cases where sample lifetimes are too short, particle sizes too great, and/or multiple time scales of motion exist that cause broadening of the solution NMR spectra at typical data collection conditions.

The membrane proteins that we are interested in are integral membrane proteins: DsbB and cytochrome bo_3 (cyt bo_3). DsbB (20 kDa) is responsible to reoxidize the periplasmic protein DsbA (21 kDa) to form a disulfide bond generation and transfer pathway that catalyzes protein folding in *E. coli* periplasm.[24,25] Although DsbA/DsbB is not found in humans, its presence and role in the folding of virulence factors in several pathogenic bacteria make these proteins a potential target for therapeutics.[26,27] Cyt bo_3 is an

integral MP that is the major terminal oxidase in the *E. coli* respiratory chain. The enzyme catalyzes the oxidation of ubiquinol and reduction of oxygen to water, and pumps protons across the membrane to generate a proton motive force. Cyt bo_3 has a molecular weight of 144 kDa, contains four subunits and 23 transmembrane helices, and is a member of the heme/copper oxidase superfamily.[28,29] DsbB and cyt bo_3 share the same cofactor, ubiquinone (UQ-8), and thus, the structural studies of the ubiquinone binding sites of DsbB and cytochrome bo_3 provide insights into the redox states and interactions of ubiquinone with these MPs.

Improvement of Sensitivity and Resolution in SSNMR Spectra of Membrane Proteins. We have established protocols for a variety of isotopic labeling methods in the context of our MP targets: uniform ^{13}C ^{15}N; checkerboard with 1,3-^{13}C-glycerol or 2-^{13}C-glycerol; "reverse" labeling to omit certain amino acids; amino-acid specific labeling with and without the use of *E. coli* auxotrophs; and adaptation of the method of Marley et al.[30] where cell pregrowth occurs in rich medium and then cells are resuspended at 4× concentration in labeling medium to increase expression yields. In addition, we have engineered a complete set of *E. coli* C43 (DE3) auxotrophs for amino acid specific labeling of MPs,[31] as well as specific labeling of ubiquinone, a cofactor for both bo_3 oxidase and DsbB. We increased purity of DsbB using one-column affinity purification from <70% to >90% purity by centrifugation and dialysis. Contaminating protein and lipids are removed, leaving still-soluble DsbB in the supernatant. We can precisely and reproducibly remove detergent from these preparations using methyl-β-cyclodextrin, which binds dodecylmaltoside (and other detergents) at a 1:1 ratio. After detergent removal, our samples of DsbB and cyt bo_3 retain 25−50 mol of phospholipid per mole of protein, and both UV−vis and SSNMR spectra are consistent with the protein in its native conformation.[32] We determine cyt bo_3 activity before and after NMR, by the method of Ma et al.,[33] and assess quinone content by the HPLC method of Rumbley et al.[34] The SSNMR preparations are highly similar to those used for FTIR and EPR studies by Gennis. For DsbB, not all preparations exhibit turnover or electron transfer to the UQ-8. For instance, the wild-type (WT) DsbB preparations are active, and mutants trapping kinetic intermediates exhibit prominent ∼500 nm absorbance (Figure 3B) consistent with those studied by the Bardwell lab and others;[35] we follow this charge-transfer band as an indication of the proper folding, assembly, and coordination of the active site.

Assignment and Interpretation of Specific Sites of Functional Interest. Our high-quality MP samples have allowed us to complete many site-specific chemical shift assignments. For example, the majority of the transmembrane helical portions of DsbB (20 kDa) have been assigned using 3D experiments on uniformly labeled samples.[36,37] We have observed unique patterns of cross-peaks between methyl and aromatic groups in several 2D DARR spectra of DsbB, attributed to the UQ. Two dimensional double-quantum (DQ) experiments were performed to isolate specific one-bond and two-bond correlations (Figure 3A). This is especially interesting, since it is often the case that in either X-ray crystallographic or solution NMR structural studies of DsbB that a UQ binding site is empty or only partially occupied, or is reconstituted with a more hydrophilic UQ-2. In contrast, the SSNMR sample preparation requires no such reconstitution providing endogenous information about the UQ-8 (Figure 3A) in its natural binding site. Through our studies of UQ-8 in DsbB, we have observed a distinctive chemical shift change stemming from the UQ-8 carbonyls when lowering the pH from 8.0 to 5.5 (Figure 3C). The chemical shift change is consistent with the protonation of the DsbB-C44 thiolate below pH 6.8 and thus provides direct evidence of the charge-transfer complex formation (Figure 3D).[32] We have also optimized chemical shift assignment strategies using DsbB's soluble protein partner DsbA in nanocrystalline preparations.[38] Greater than 90% of the backbone resonances have been assigned with optimized isotopic labeling strategies and 3D/4D spectroscopy optimized for resolution and sensitivity.[39] We also have $^{15}N-^{13}C$ correlation experiments on specific amino acid labeled cyt bo_3 samples,[31] which will lead toward the assignment of the ^{288}YILIL segment near the reaction center in cyt bo_3.

High Resolution Structure of a Membrane Protein. We employed sparse isotopic labeling with 2-^{13}C- or 1,3-^{13}C-glycerol[40] to obtain distance restraints from 2D $^{13}C-^{13}C$ correlation experiments. The labeling scheme yields [2-^{13}C-glycerol,^{15}N]DsbB (2-DsbB) with mainly Cα atoms ^{13}C labeled and [1,3-^{13}C-glycerol,^{15}N]DsbB (1,3-DsbB) with CO and methylene/methyl atoms ^{13}C labeled, which greatly reduces the degeneracy of the cross-peaks and avoids the J-couplings between directly bonded ^{13}C labels. We were able to extract long-range distance restraints, including some unambiguous and many ambiguous long-range distance restraints. Combining the SSNMR restraints of $^{13}C-^{13}C$ distances and dihedral angles with X-ray reflections obtained from the protein data bank, we performed joint

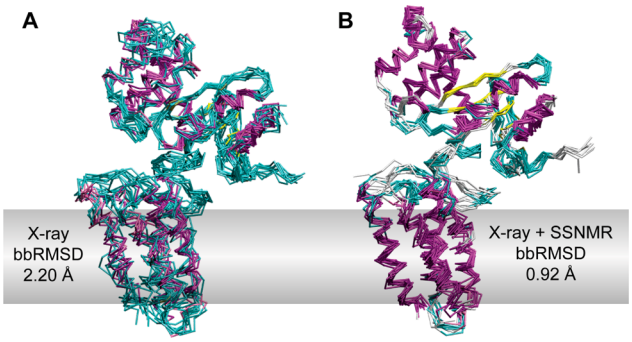

FIGURE 4. High-resolution structure of DsbB-DsbA.[42] Overlay of 10 lowest-energy structures of DsbB-DsbA, calculated against (A) only X-ray reflections and (B) X-ray reflections and SSNMR restraints. The colors represent the secondary structure elements (magenta: α-helix, cyan and white: coil and turn, yellow: β-strand). The gray band indicates the membrane. The bbRMSD of the transmembrane regions are labeled. Adapted with permission from ref 42. Copyright 2011 Springer Science + Business Media.

refinement of the DsbA-DsbB structure using XPLOR-NIH simulated annealing.[41] The commonly used potential terms of bonds, angles, improper torsions, van der Waals, hydrogen bonds, NOEs ($^{13}C-^{13}C$ distances), and dihedral angles (TALOS+ restraints) were included along with a specific potential term for direct refinement against crystallographic structure factors. So far, the overall bbRMSD was improved from 1.63 Å (X-ray) to 1.02 Å (X-ray and SSNMR data).[42] In the TM helices of DsbB, bbRMSD improvement is ~50% over the X-ray data alone (Figure 4), due to the fact that isotropic N, CA, and CB chemical shift information provides good helical restraints. This method is suitable for large MP systems, in which X-ray crystallography or NMR cannot provide high-resolution structures alone.

Amyloid Fibrils

Parkinson's disease (PD) is the second most common neurodegenerative disease and one of the 15 most common causes of death in the United States.[43] PD is pathologically characterized by the presence of Lewy bodies (LB), aggregates found in the dopaminergic neurons during patients autopsy.[44] In 1997, Spillantini et al. discovered that the main component of LB is fibrillar $\alpha-$synuclein (AS).[45] Subsequent studies demonstrated that AS in unstructured in solution[46] and it binds to anionic phospholipids with an α-helical secondary structure.[47] While most cases of PD are sporadic, three distinct mutations (A30P, E46K, A53T) in the AS gene[48−50] have been identified in familial early onset PD. Although all these findings implicate AS misfolding in PD and have motivate numerous investigations to understand the fibrils formation, up to now no high resolution structure has yet been published. MAS SSNMR spectroscopy provides high-resolution structural information of amyloidogenic fibrils, which are not accessible by traditional biophysical methods of solution NMR and X-ray diffraction.

Assignment and Secondary Structure of AS Fibrils. Due to the significant biomedical relevance of AS fibrils and complexity for its structural study, the solid-state NMR community has been extensively studied them.[51−55] Our early investigations focused on the expression, purification (Figure 5A), and fibril preparation by carefully controlling the incubation conditions and demonstrating reproducible sample preparation.[56] This was an essential prerequisite for using different labeling schemes and investigating the structural perturbation by mutation or in the presence of lipids. Since our initial studies, significant improvement in the spectral resolution and sensitivity was accomplished by modification of the sample hydration. Our first samples were prepared by ultracentrifuging the mature fibrils, removing the supernatant and packing the hydrated pellet in the SSNMR rotor. This sample preparation led to lower intensity in the cross-polarization (CP)-based ^{13}C spectra than expected for a 14 kDa protein (CP enhancement factor of ~0.7). By lowering the temperature, significant CP enhancement was obtained, which approximated the low order parameters behavior from $^{1}H-^{13}C$ dipolar dephasing curves acquired with the $R18_1^7$ sequence (Figure 5B).[57] These results were attributed to the freezing of the mother liquor. Although increased spectral intensity made possible assignment of ~48% of all ^{13}C and ^{15}N resonances between residues 38 and 96, further assignment progress was significantly challenging,[52,58] even with the use of 4D heteronuclear experiments.[15] Further sensitivity enhancement was accomplished by drying the fibrils and attributed to the increase in sample rigidity (CP enhancement factor of ~2.0) and to the amount of fibrils packed in the SSNMR rotor, as water previously occupied a substantial part of it. Almost identical chemical shifts were obtained when compared to the hydrated samples (Figure 5C), suggesting no perturbations in the fibril structure.[59] Our recent progress has demonstrated that drying and rehydrating the fibrils leads to optimal spectral sensitivity and resolution.[54] By combining optimized sample preparation with sparse isotopic labeling schemes, and state-of the art SSNMR experiments, we have detected additional residues and obtained comprehensive chemical shift assignments for the backbone and side chain resonances of the fibril core (~91% of all resonances between residues 38 and 97).[54] These results demonstrated that the core of the fibrils extends with a repeated secondary structure motif (Figure 5E). A systematic conformational

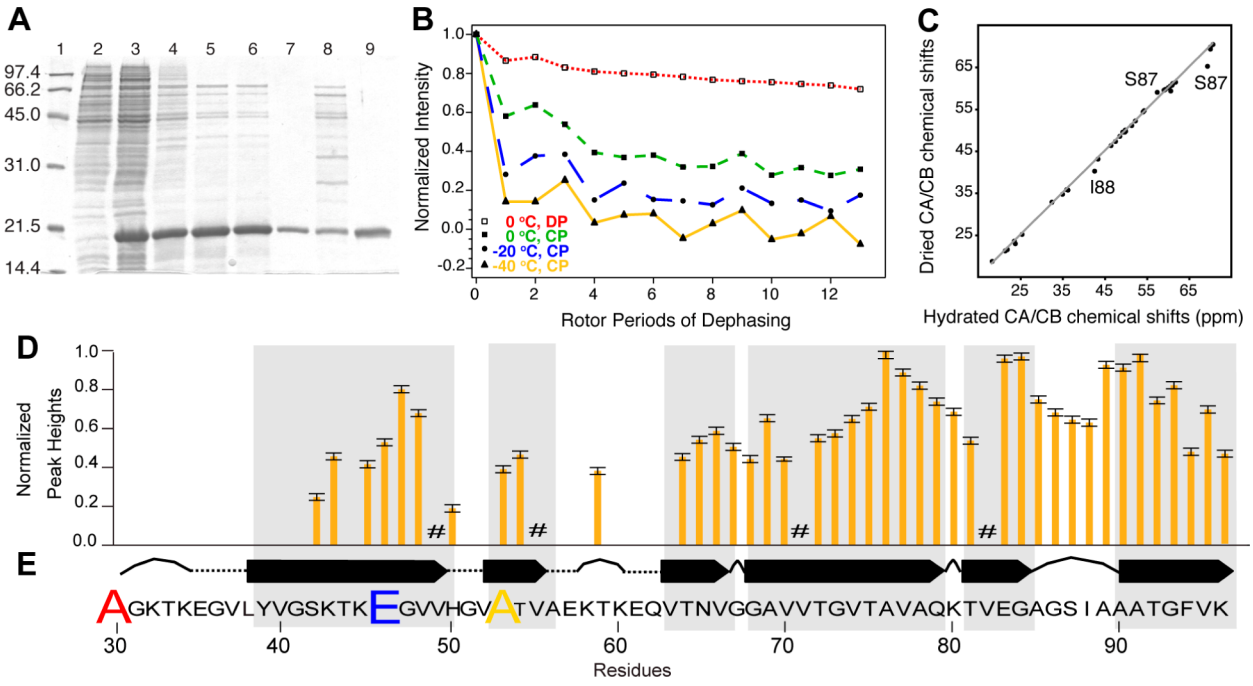

FIGURE 5. Solid-state NMR reveals site-specific structural and conformational details of the AS fibril structure and its formation. (A) SDS-page analysis of a representative purification of AS.[56] (B) $^{1}H-^{13}C$ dipolar dephasing curves for AS fibrils at different variable temperatures using the $R18_1^7$ pulse sequence.[52] (C) Correlation of chemical shifts between hydrated and dried fibrils.[59] (D) Relative peak heights from the cross-peaks of the 3D CANCO spectrum of $U-^{13}C,^{15}N$ AS fibrils.[54] (E) Representation of the secondary structure of AS fibrils.[54] Adapted with permission from refs 56, 52, 59, and 54. Copyright 2006 Elsevier Inc., 2007 Springer Science + Business Media, 2007 American Chemical Society, and 2011 Elsevier Inc., respectively.

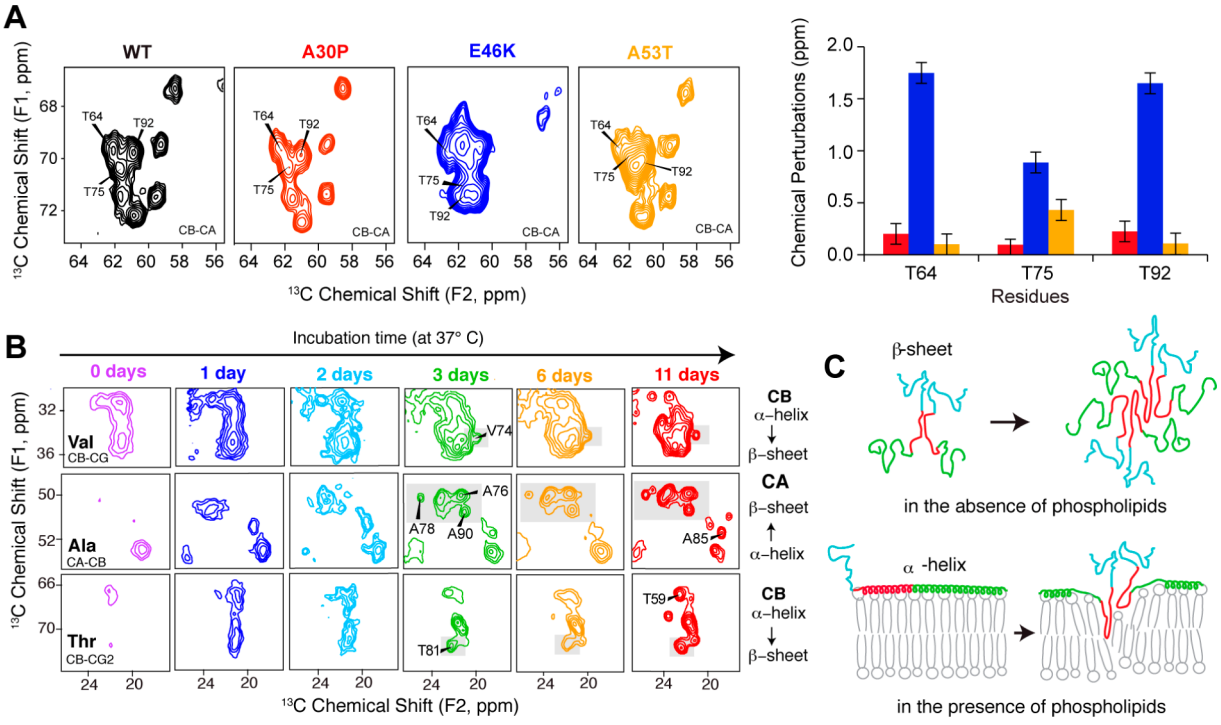

FIGURE 6. AS mutants and AS-membrane interactions. (A) Spectral comparison and chemical shift comparison of the WT and the three early onset PD mutants.[54,63] (B) Transition from α-helix to β-sheet evidenced by the changes in chemical shifts of AS incubated in the presence of phospholipids. (C) Schematic representation of the proposed mechanism of AS fibril formation in the absence and the presence of phospholipids.[64] Adapted with permission from refs 54 and 64. Copyright 2011 Elsevier Inc. and 2012 American Chemical Society, respectively.

dynamic study also revealed that some of these residues, not previously detected, are located in β-strand regions that impact the fibril structure. In fact, these results disagree with the previously proposed fold of AS fibrils obtained with limited SSNMR data.[60] In addition, they demonstrate that the essential residues for the fibril formation, described by Giasson et al.,[61] are within the most stable residues in the fibril state (Figure 5D).

AS Mutants and AS−Membrane Interactions. Bax and co-workers reported differences in the lipid binding modes of early onset PD AS mutants (A30P, E46K, A53T) and proposed possible differences in their fibrillation pathways.[62] In this direction, our structural studies have demonstrated that the three mutation sites (A30, E46, A53) are located in structured regions for the WT fibrils.[54] In order to investigate the possible differences, fibrils for the three single point mutants were prepared and their chemical shifts were de novo assigned. These results demonstrate major and minor chemical shift perturbations by E46K and A53T, respectively; while they are practically unaltered by A30P (Figure 6A).[63] In the case of E46K, the perturbations are spread in the core, while those for A53T are focused near the mutation site, the 60s and 80s and for A30P only near the 60s. Although these results provide site-specific structural information of the fibrils from three mutants, further examination of the AS mutant fibrillogenesis will be required to understand their role in the disease. To do so, we have recently captured the transition from α-helical to β-sheet of WT AS in the presence of phospholipid vesicles (Figure 6B). We have compared the fibrillations in the presence and absence of lipids and proposed the differences in their mechanisms (Figure 6C).[64] In addition, our results demonstrate that the residues described to be essential for the fibril formation[61] are the ones that are initially stabilized in the presence of lipids.

Concluding Remarks

The advancements in SSNMR methods have provided new ways to investigate difficult protein targets. Although the development of SSNMR methods, in particular multidimensional MAS methods, to study large proteins have emerged only recently (relative to crystallography and solution NMR), SSNMR technology has advanced considerably in the past decade and now is ready to tackle major challenges with respect to protein structure determination. Beyond the emerging ability of SSNMR to solve complete structures, there is significant potential in terms of joint refinement of X-ray reflections and SSNMR restraints. We have extended these methodologies to situations where low- and medium-resolution X-ray data can be combined with SSNMR derived high-resolution restraints.[42] This seems likely to be a general capability, since high-quality SSNMR spectra can be collected on nano- or microcrystals, as well as noncrystalline membrane proteins. The structure of DsbB and the structural changes at the UQ-binding site from SSNMR can provide an understanding of the chemistry that takes place to facilitate electron transfer and disulfide bond formation.

Current ongoing efforts toward a high-resolution 3D structure of AS fibrils include, for example, our recent investigations involving thiol-ligated paramagnetic spin labels to provide further restraints of the fibril arrangement. This methodology has recently been demonstrated to be successful to achieve the GB1 protein fold.[65] We believe that having further high-resolution structural information of AS fibrils will help in understanding how the fibrils lead to the formation of Lewy bodies or the possible role of the early onset PD mutants.

The authors acknowledge generous support from the National Science Foundation (MCB0347824 to C.M.R.), the National Institutes of Health (R01GM075937, R01GM073770, R01HL103999, and S10RR025037 to C.M.R.), and fellowship support to G.C. from Caja Madrid and Agusti Pedro Pons Foundations.

BIOGRAPHICAL INFORMATION

Ming Tang received his B.S. in chemistry from Peking University (Beijing, China) in 2003. He received his Ph.D. in 2008 from Iowa State University. His graduate research with Prof. Mei Hong focused on the SSNMR study of antimicrobial peptides. His current postdoctoral research is studying membrane proteins using multidimensional SSNMR techniques with Prof. Chad Rienstra at the University of Illinois at Urbana−Champaign.

Gemma Comellas was born in Berga (Barcelona, Spain) in 1984. She received her B.S. in chemistry from the University of Barcelona in 2006, performing undergraduate research in the laboratory of Prof. R. Lee Penn at the University of Minnesota at Twin-Cities. In 2007, she obtained a M.S. in chemistry from the University of Barcelona under the supervision of Prof. Ernest Giralt, and in 2012 a Ph.D. in Biophysics and Computational Biology from the University of Illinois at Urbana−Champaign under the guidance of Prof. Chad Rienstra. During her dissertation work, she pursued SSNMR structural and dynamic studies of α-synuclein fibrils.

Chad M. Rienstra received his B.A. degree in chemistry from Macalester College (St. Paul, MN) in 1993 and his Ph.D. at the Massachusetts Institute of Technology in 1999. He was a postdoctoral fellow at Columbia University. He is an Associate Professor of Chemistry at the University of Illinois at Urbana−Champaign. His research interests are in SSNMR, including the development of new pulse sequence methodology and instrumentation, and application to studies of protein structure and dynamics.

FOOTNOTES

*To whom correspondence should be addressed. E-mail: rienstra@illinois.edu.
The authors declare no competing financial interest.

REFERENCES

1 Franks, W. T.; Wylie, B. J.; Stellfox, S. A.; Rienstra, C. M. Backbone conformational constraints in a microcrystalline U-^{15}N-labeled protein by 3D dipolar-shift solid-state NMR spectroscopy. *J. Am. Chem. Soc.* **2006**, *128*, 3154–3155.

2 Wylie, B. J.; Schwieters, C. D.; Oldfield, E.; Rienstra, C. M. Protein Structure Refinement Using 13Cα Chemical Shift Tensors. *J. Am. Chem. Soc.* **2009**, *131*, 985–992.

3 Franks, W. T.; Kloepper, K. D.; Wylie, B. J.; Rienstra, C. M. Four-dimensional heteronuclear correlation experiments for chemical shift assignment of solid proteins. *J. Biomol. NMR* **2007**, *39*, 107–131.

4 Franks, W. T.; Wylie, B. J.; Schmidt, H. L. F.; Nieuwkoop, A. J.; Mayrhofer, R. M.; Shah, G. J.; Graesser, D. T.; Rienstra, C. M. Dipole tensor-based atomic-resolution structure determination of a nanocrystalline protein by solid-state NMR. *Proc. Natl. Acad. Sci. U.S.A.* **2008**, *105*, 4621–4626.

5 Wylie, B. J.; Franks, T.; Graesser, D. T.; Rienstra, C. M. Site-specific ^{13}C chemical shift anisotropy measurements in a uniformly ^{15}N,^{13}C-labeled microcrystalline protein by 3D magic-angle spinning NMR spectroscopy. *J. Am. Chem. Soc.* **2005**, *127*, 11946–11947.

6 Wylie, B. J.; Franks, W. T.; Rienstra, C. M. Determinations of ^{15}N chemical shift anisotropy magnitudes in a uniformly ^{15}N,^{13}C-labeled microcrystalline protein by three-dimensional magic-angle spinning nuclear magnetic resonance spectroscopy. *J. Phys. Chem. A* **2006**, *110*, 10926–10936.

7 Wylie, B. J.; Rienstra, C. M. Multidimensional solid state NMR of anisotropic interactions in peptides and proteins. *J. Chem. Phys.* **2008**, *128*, 052207.

8 Wylie, B. J.; Sperling, L. J.; Nieuwkoop, A. J.; Franks, W. T.; Oldfield, E.; Rienstra, C. M. Ultrahigh resolution protein structures using NMR chemical shift tensors. *Proc. Natl. Acad. Sci. U.S.A.* **2011**, *108*, 16974–16979.

9 Nieuwkoop, A. J.; Wylie, B. J.; Franks, W. T.; Shah, G. J.; Rienstra, C. M. Atomic resolution protein structure determination by three-dimensional transferred echo double resonance solid-state nuclear magnetic resonance spectroscopy. *J. Chem. Phys.* **2009**, *131*, 095101.

10 Zhou, D. H.; Rienstra, C. M. High-performance solvent suppression for proton detected solid-state NMR. *J. Magn. Reson.* **2008**, *192*, 167–172.

11 Zhou, D. H.; Shah, G.; Cormos, M.; Mullen, C.; Sandoz, D.; Rienstra, C. M. Proton-detected solid-state NMR spectroscopy of fully protonated proteins at 40 kHz magic-angle spinning. *J. Am. Chem. Soc.* **2007**, *129*, 11791–11801.

12 Zhou, D. H.; Shah, G.; Mullen, C.; Sandoz, D.; Rienstra, C. M. Proton-Detected Solid-State NMR Spectroscopy of Natural-Abundance Peptide and Protein Pharmaceuticals. *Angew. Chem., Int. Ed.* **2009**, *48*, 1253–1256.

13 Zhou, D. H.; Shea, J. J.; Nieuwkoop, A. J.; Franks, W. T.; Wylie, B. J.; Mullen, C.; Sandoz, D.; Rienstra, C. M. Solid-state protein-structure determination with proton-detected triple-resonance 3D magic-angle-spinning NMR spectroscopy. *Angew. Chem., Int. Ed.* **2007**, *46*, 8380–8383.

14 Zhou, D. H.; Nieuwkoop, A. J.; Berthold, D. A.; Comellas, G.; Sperling, L. J.; Tang, M.; Shah, G. J.; Brea, E. J.; Lemkau, L. R.; Rienstra, C. M. Solid-state NMR analysis of membrane proteins and protein aggregates by proton detected spectroscopy. *J. Biomol. NMR* **2012**, *54*, 291–305.

15 Cornilescu, G.; Delaglio, F.; Bax, A. Protein backbone angle restraints from searching a database for chemical shift and sequence homology. *J. Biomol. NMR* **1999**, *13*, 289–302.

16 Overington, J. P.; Al-Lazikani, B.; Hopkins, A. L. How many drug targets are there? *Nat. Rev. Drug Discovery* **2006**, *5*, 993–996.

17 Carpenter, E. P.; Beis, K.; Cameron, A. D.; Iwata, S. Overcoming the challenges of membrane protein crystallography. *Curr. Opin. Struct. Biol.* **2008**, *18*, 581–586.

18 White, S. H. The progress of membrane protein structure determination. *Protein Sci.* **2004**, *13*, 1948–1949.

19 Lacapere, J. J.; Pebay-Peyroula, E.; Neumann, J. M.; Etchebest, C. Determining membrane protein structures: still a challenge!. *Trends Biochem. Sci.* **2007**, *32*, 259–270.

20 Loll, P. J. Membrane protein structural biology: the high throughput challenge. *J. Struct. Biol.* **2003**, *142*, 144–153.

21 Li, M.; Hays, F. A.; Roe-Zurz, Z.; Vuong, L.; Kelly, L.; Ho, C. M.; Robbins, R. M.; Pieper, U.; O'Connell, J. D., 3rd; Miercke, L. J.; Giacomini, K. M.; Sali, A.; Stroud, R. M. Selecting optimum eukaryotic integral membrane proteins for structure determination by rapid expression and solubilization screening. *J. Mol. Biol.* **2009**, *385*, 820–830.

22 Wiener, M. C. A pedestrian guide to membrane protein crystallization. *Methods* **2004**, *34*, 364–372.

23 Newby, Z. E.; O'Connell, J. D., 3rd; Gruswitz, F.; Hays, F. A.; Harries, W. E.; Harwood, I. M.; Ho, J. D.; Lee, J. K.; Savage, D. F.; Miercke, L. J.; Stroud, R. M. A general protocol for the crystallization of membrane proteins for X-ray structural investigation. *Nat. Protoc.* **2009**, *4*, 619–637.

24 Kadokura, H.; Katzen, F.; Beckwith, J. Protein disulfide bond formation in prokaryotes. *Annu. Rev. Biochem.* **2003**, *72*, 111–135.

25 Messens, J.; Collet, J. F. Pathways of disulfide bond formation in Escherichia coli. *Int. J. Biochem. Cell Biol.* **2006**, *38*, 1050–1062.

26 Łasica, A. M.; Jagusztyn-Krynicka, E. K. The role of Dsb proteins of Gram-negative bacteria in the process of pathogenesis. *FEMS Microbiol. Rev.* **2007**, *31*, 626–636.

27 Heras, B.; Kurz, M.; Jarrott, R.; Shouldice, S. R.; Frei, P.; Robin, G.; Cemazar, M.; Thony-Meyer, L.; Glockshuber, R.; Martin, J. L. Staphylococcus aureus DsbA does not have a destabilizing disulfide - A new paradigm for bacterial oxidative folding. *J. Biol. Chem.* **2008**, *283*, 4261–4271.

28 Garcia-Horsman, J. A.; Barquera, B.; Rumbley, J.; Ma, J. X.; Gennis, R. B. The superfamily of heme-copper respiratory oxidases. *J. Bacteriol.* **1994**, *176*, 5587–5600.

29 Pereira, M. M.; Santana, M.; Teixeira, M. A novel scenario for the evolution of haem-copper oxygen reductases. *Biochim. Biophys. Acta, Bioenerg.* **2001**, *1505*, 185–208.

30 Marley, J.; Lu, M.; Bracken, C. A method for efficient isotopic labeling of recombinant proteins. *J. Biomol. NMR* **2001**, *20*, 71–75.

31 Lin, M. T.; Sperling, L. J.; Frericks Schmidt, H. L.; Tang, M.; Samoilova, R. I.; Kumasaka, T.; Iwasaki, T.; Dikanov, S. A.; Rienstra, C. M.; Gennis, R. B. A rapid and robust method for selective isotope labeling of proteins. *Methods* **2011**, *55*, 370–378.

32 Tang, M.; Sperling, L. J.; Berthold, D. A.; Nesbitt, A. E.; Gennis, R. B.; Rienstra, C. M. Solid-state NMR study of the charge-transfer complex between ubiquinone-8 and disulfide bond generating membrane protein DsbB. *J. Am. Chem. Soc.* **2011**, *133*, 4359–4366.

33 Ma, J. X.; Puustinen, A.; Wikstrom, M.; Gennis, R. B. Tryptophan-136 in subunit II of cytochrome bo(3) from Escherichia coli may participate in the binding of ubiquinol. *Biochemistry* **1998**, *37*, 11806–11811.

34 Rumbley, J. N.; Nickels, E. F.; Gennis, R. B. One-step purification of histidine-tagged cytochrome bo(3) from Escherichia coli and demonstration that associated quinone is not required for the structural integrity of the oxidase. *Biochim. Biophys. Acta, Protein Struct. Mol. Enzymol.* **1997**, *1340*, 131–142.

35 Tapley, T. L.; Eichner, T.; Gleiter, S.; Ballou, D. P.; Bardwell, J. C. A. Kinetic characterization of the disulfide bond-forming enzyme DsbB. *J. Biol. Chem.* **2007**, *282*, 10263–10271.

36 Li, Y.; Berthold, D. A.; Frericks, H. L.; Gennis, R. B.; Rienstra, C. M. Partial C-13 and N-15 chemical-shift assignments of the disulfide-bond-forming enzyme DsbB by 3D magic-angle spinning NMR spectroscopy. *ChemBioChem* **2007**, *8*, 434–442.

37 Li, Y.; Berthold, D. A.; Gennis, R. B.; Rienstra, C. M. Chemical shift assignment of the transmembrane helices of DsbB, a 20-kDa integral membrane enzyme, by 3D magic-angle spinning NMR spectroscopy. *Protein Sci.* **2008**, *17*, 199–204.

38 Sperling, L. J.; Nieuwkoop, A. J.; Lipton, A. S.; Berthold, D. A.; Rienstra, C. M. High resolution NMR spectroscopy of nanocrystalline proteins at ultra-high magnetic field. *J. Biomol. NMR* **2010**, *46*, 149–155.

39 Sperling, L. J.; Berthold, D. A.; Sasser, T. L.; Jeisy-Scott, V.; Rienstra, C. M. Assignment strategies for large proteins by magic-angle spinning NMR: the 21-kDa disulfide bond forming enzyme DsbA. *J. Mol. Biol.* **2010**, *399*, 268–282.

40 Castellani, F.; van Rossum, B.; Diehl, A.; Schubert, M.; Rehbein, K.; Oschkinat, H. Structure of a protein determined by solid-state magic-angle- spinning NMR spectroscopy. *Nature* **2002**, *420*, 98–102.

41 Schwieters, C. D.; Kuszewski, J. J.; Tjandra, N.; Clore, G. M. The Xplor-NIH NMR molecular structure determination package. *J. Magn. Reson.* **2003**, *160*, 65–73.

42 Tang, M.; Sperling, L. J.; Berthold, D. A.; Schwieters, C. D.; Nesbitt, A. E.; Nieuwkoop, A. J.; Gennis, R. B.; Rienstra, C. M. High-resolution membrane protein structure by joint calculations with solid-state NMR and X-ray experimental data. *J. Biomol. NMR* **2011**, *51*, 227–133.

43 Kochanek, K.; Xu, J.; Murphy, S.; Minino, A.; Kung, H. Deaths: preliminary data for 2009. *Natl. Vital Stat. Rep.* **2012**, *59*, 1–51.

44 Lewy, F. H. Pathologische Anatomie. In *Hundbuch der Neurologie*; Lewandowsky, M., Ed.; Springer-Verlag: Berlin, Germany, 1912; pp 920−933.

45 Spillantini, M. G.; Schmidt, M. L.; Lee, V. M. Y.; Trojanowski, J. Q.; Jakes, R.; Goedert, M. alpha-Synuclein in Lewy bodies. *Nature* **1997**, *388*, 839–840.

46 Eliezer, D.; Kutluay, E.; Bussell, R.; Browne, G. Conformational properties of alpha-synuclein in its free and lipid-associated states. *J. Mol. Biol.* **2001**, *307*, 1061–1073.

47 Perrin, R. J.; Woods, W. S.; Clayton, D. F.; George, J. M. Interaction of human alpha-synuclein and Parkinson's disease variants with phospholipids - Structural analysis using site- directed mutagenesis. *J. Biol. Chem.* **2000**, *275*, 34393–34398.

48 Polymeropoulos, M. H.; Lavedan, C.; Leroy, E.; Ide, S. E.; Dehejia, A.; Dutra, A.; Pike, B.; Root, H.; Rubenstein, J.; Boyer, R.; Stenroos, E. S.; Chandrasekharappa, S.; Athanassiadou, A.; Papapetropoulos, T.; Johnson, W. G.; Lazzarini, A. M.; Duvoisin, R. C.; Dilorio, G.; Golbe, L. I.; Nussbaum, R. L. Mutation in the alpha-synuclein gene identified in families with Parkinson's disease. *Science* **1997**, *276*, 2045–2047.

49 Kruger, R.; Kuhn, W.; Muller, T.; Woitalla, D.; Graeber, M.; Kosel, S.; Przuntek, H.; Epplen, J. T.; Schols, L.; Riess, O. Ala30Pro mutation in the gene encoding alpha-synuclein in Parkinson's disease. *Nat. Genet.* **1998**, *18*, 106–108.

50 Zarranz, J. J.; Alegre, J.; Gomez-Esteban, J. C.; Lezcano, E.; Ros, R.; Ampuero, I.; Vidal, L.; Hoenicka, J.; Rodriguez, O.; Atares, B.; Llorens, V.; Tortosa, E. G.; del Ser, T.; Munoz, D. G.; de Yebenes, J. G. The new mutation, E46K, of alpha-synuclein causes Parkinson and Lewy body dementia. *Ann. Neurol.* **2004**, *55*, 164–173.

51 Heise, H.; Hoyer, W.; Becker, S.; Andronesi, O. C.; Riedel, D.; Baldus, M. Molecular-level secondary structure, polymorphism, and dynamics of full-length alpha-synuclein fibrils studied by solid-state NMR. *Proc. Natl. Acad. Sci. U.S.A.* **2005**, *102*, 15871–15876.

52 Kloepper, K. D.; Zhou, D. H.; Li, Y.; Winter, K. A.; George, J. M.; Rienstra, C. M. Temperature-dependent sensitivity enhancement of solid-state NMR spectra of alpha-synuclein fibrils. *J. Biomol. NMR* **2007**, *39*, 197–211.

53 Loquet, A.; Giller, K.; Becker, S.; Lange, A. Supramolecular interactions probed by 13C-13C solid-state NMR spectroscopy. *J. Am. Chem. Soc.* **2010**, *132*, 15164–15166.

54 Comellas, G.; Lemkau, L. R.; Nieuwkoop, A. J.; Kloepper, K. D.; Ladror, D. T.; Ebisu, R.; Woods, W. S.; Lipton, A. S.; George, J. M.; Rienstra, C. M. Structured regions of alpha-synuclein fibrils include the early-onset Parkinson's disease mutation sites. *J. Mol. Biol.* **2011**, *411*, 881–895.

55 Gath, J.; Habenstein, B.; Bousset, L.; Melki, R.; Meier, B. H.; Bockmann, A. Solid-state NMR sequential assignments of alpha-synuclein. *Biomol. NMR Assignments* **2012**, *6*, 51–55.

56 Kloepper, K. D.; Woods, W. S.; Winter, K. A.; George, J. M.; Rienstra, C. M. Preparation of alpha-synuclein fibrils for solid-state NMR: Expression, purification, and incubation of wild-type and mutant forms. *Protein Expression Purif.* **2006**, *48*, 112–117.

57 Zhao, X.; Eden, M.; Levitt, M. H. Recoupling of heteronuclear dipolar interactions in solid-state NMR using symmetry-based pulse sequences. *Chem. Phys. Lett.* **2001**, *342*, 353–361.

58 Zhou, D. H.; Kloepper, K. D.; Winter, K. A.; Rienstra, C. M. Band-selective ^{13}C homonuclear 3D spectroscopy for solid proteins at high field with rotor-synchronized soft pulses. *J. Biomol. NMR* **2006**, *34*, 245–257.

59 Kloepper, K. D.; Hartman, K. L.; Ladror, D. T.; Rienstra, C. M. Solid-state NMR spectroscopy reveals that water is nonessential to the core structure of alpha-synuclein fibrils. *J. Phys. Chem. B* **2007**, *111*, 13353–13356.

60 Vilar, M.; Chou, H.-T.; Luhrs, T.; Samir, M.; Riek-Loher, D.; Verel, R.; Manning, G.; Stahlberg, H.; Riek, R. The fold of alpha-synuclein fibrils. *Proc. Natl. Acad. Sci. U.S.A.* **2008**, *105*, 8637–8642.

61 Giasson, B. I.; Murray, I. V. J.; Trojanowski, J. Q.; Lee, V. M. Y. A hydrophobic stretch of 12 amino acid residues in the middle of alpha-synuclein is essential for filament assembly. *J. Biol. Chem.* **2001**, *276*, 2380–2386.

62 Bodner, C. R.; Maltsev, A. S.; Dobson, C. M.; Bax, A. Differential Phospholipid Binding of alpha-Synuclein Variants Implicated in Parkinson's Disease Revealed by Solution NMR Spectroscopy. *Biochemistry* **2010**, *49*, 862–871.

63 Lemkau, L. R.; Comellas, G.; Kloepper, K. D.; Woods, W. S.; George, J. M.; Rienstra, C. M. Mutant protein A30P alpha-synuclein adopts wild-type fibril structure, despite slower fibrillation kinetics. *J. Biol. Chem.* **2012**, *287*, 11526–11532.

64 Comellas, G.; Lemkau, L. R.; Zhou, D. H.; George, J. M.; Rienstra, C. M. Structural intermediates during alpha-synuclein fibrillogenesis on phospholipid vesicles. *J. Am. Chem. Soc.* **2012**, *134*, 5090–5099.

65 Sengupta, I.; Nadaud, P. S.; Helmus, J. J.; Schwieters, C. D.; Jaroniec, C. P. Protein fold determined by paramagnetic magic-angle spinning solid-state NMR spectroscopy. *Nat. Chem.* **2012**, *4*, 410–417.